

Measuring Dark Matter Power Spectrum from Cosmic Microwave Background

Uroš Seljak*†

Max-Planck Institut fuer Astrophysik, Karl-Schwartzschild-Str. 1, 85740 Garching beim Muenchen, Germany

Matias Zaldarriaga‡

Institute for Advanced Studies, School of Natural Sciences, Princeton, NJ 08540

(October 1998)

We propose a method to extract the projected power spectrum of density perturbations from the distortions in the cosmic microwave background (CMB). The distortions are imprinted onto the CMB by the gravitational lensing effect and can be extracted using a combination of products of CMB derivatives. We show that future CMB experiments such as Planck will be able to extract the power spectrum with high statistical significance over two orders of magnitude in angle. The method proposed here traces dark matter directly to higher redshift (up to $z \sim 1100$) and larger scale (few Gpc) than any other currently known method. It also traces large scale structure in the linear regime, allowing simple interpretation in terms of cosmological models. By providing additional and complementary information to the one from the primary CMB analysis it will strengthen further the scientific return of future CMB experiments.

PACS numbers: 98.80.Es, 95.85.Bh, 98.35.Ce, 98.70.Vc

The standard paradigm of modern cosmology is the expanding universe model, where the universe started with a hot big bang and has been expanding ever since. The universe is predicted to be homogeneous and isotropic on large scales with initially small fluctuations superimposed on that background. These fluctuations have been amplified by gravity to become the present day large scale structure. This paradigm, while successful in explaining all the observations, still leaves many questions unanswered. Among these are the value of cosmological parameters, such as the density of the various components, the nature of dark matter and the power spectrum of initial perturbations.

Observational efforts are necessary to provide the answers to the above questions. It has long been recognized that the power spectrum of dark matter fluctuations would provide many of these answers, as it depends both on the initial power spectrum as well as on the rate of growth of perturbations, which are determined by the cosmological model and the nature of dark matter (e.g. hot or cold). Its measurement has been the primary target of many observational surveys in the past and this trend will also continue in the future. Most of these have used galaxy positions and redshifts to map the universe. The ongoing surveys such as SDSS and 2dF hope to measure the power spectrum accurately on scales up to several hundred megaparsecs. However, there are a number of possible uncertainties that may make this goal more difficult than expected. In particular, the fact that galaxy formation is such a poorly understood process makes the connection between mass and light uncertain. The relation between dark matter and galaxy density perturbation could be nonlinear, scale-dependent, non-local or stochastic even on very large scales [1]. Another complication is the fact that except on very large scales, the surveys are measuring the clustering in the nonlinear

regime, which makes the interpretation and statistical analysis of the data more complicated.

For these reasons other, more direct, tracers of dark matter have been investigated, most notably velocity flows [2], clustering of Ly- α forest [3] and weak lensing [4]. Each of these has uncertainties associated with them. Weak lensing, although not yet detected, offers perhaps the best chance of measuring accurately the power spectrum of dark matter over a large range of scales. By measuring the distortions in the shapes of background galaxies deformed by the mass distribution along the line of sight one can determine the clustering fluctuations on scales from 1 up to 100 h^{-1} Mpc [4–6]. Weak lensing has the advantage of tracing the dark matter directly and therefore avoids the uncertainties connected with galaxy clustering. Still, there are uncertainties associated with weak lensing as well, the most important being the poorly known redshift distribution of background galaxies and their possible intrinsic alignment.

In this letter we propose a new method to measure the projected dark matter power spectrum by using the weak lensing distortions of the CMB [7]. We show that gravitational lensing induces characteristic distortions in the pattern of the CMB field, which allows one to reconstruct the projected dark matter density field [8]. The reconstructed projected mass density can be used to measure the mass power spectrum by averaging over independent CMB patches. The method proposed here offers several advantages over the other methods discussed above. It traces the dark matter directly and does not depend on the assumptions of how light traces mass. Unlike weak lensing of galaxies it does not suffer from the possible intrinsic alignment of background galaxies or their uncertain redshift distribution. It is able to recover the power spectrum over a large range of scales, roughly between 10 Mpc and 1 Gpc. As such it is sensitive to scales

larger than any other survey, including the SDSS and 2dF. Furthermore, the observed field is a projection of density up to $z \sim 1100$ and one is therefore tracing dark matter to higher redshifts than with any other method. The last two features also imply that with the proposed method one is tracing the perturbations predominantly in the linear regime and no nonlinear corrections are necessary down to the smallest scales that are still observable. In many ways the method proposed here offers the same advantages that make the CMB anisotropies such a powerful test of cosmological models, except that it is providing complementary information on the projected dark matter power spectrum. Clearly, combining the standard CMB analysis with the present one will further enhance the power of CMB to constrain the cosmological models [9] and provide additional motivation for future CMB experiments.

To provide a clear physical interpretation we will only discuss the small scale limit of the method in this letter (see [8,10] for all-sky generalization). The observed CMB temperature in the direction $\boldsymbol{\theta}$ is $T(\boldsymbol{\theta})$ and equals the (unobservable) temperature at the last scattering surface in a different direction, $\tilde{T}(\boldsymbol{\theta} + \delta\boldsymbol{\theta})$, where $\delta\boldsymbol{\theta}$ is the angular excursion of the photon as it propagates from the last scattering surface to us. In terms of Fourier components we have $T(\boldsymbol{\theta}) = (2\pi)^{-2} \int d^2\mathbf{l} e^{i\mathbf{l}\cdot(\boldsymbol{\theta} + \delta\boldsymbol{\theta})} \tilde{T}(\mathbf{l})$. To extract the information on the deflection field $\delta\boldsymbol{\theta}$ we consider derivatives of the CMB temperature. If the CMB is an isotropic and homogeneous Gaussian random field then different partial derivatives are statistically equivalent and their spatial properties are independent of position. Lensing will distort these two properties of the derivatives. The derivatives of the temperature field are to lowest order,

$$T_a(\boldsymbol{\theta}) \equiv \frac{\partial \tilde{T}}{\partial \theta_a}(\boldsymbol{\theta} + \delta\boldsymbol{\theta}) = (\delta_{ab} + \Phi_{ab}) \tilde{T}_b(\boldsymbol{\theta} + \delta\boldsymbol{\theta}), \quad (1)$$

where $\Phi_{ab} = \frac{\partial \delta\theta_a}{\partial \theta_b}$ is the symmetric shear tensor. The components of the shear tensor can be written in terms of the convergence $\kappa = -(\Phi_{aa} + \Phi_{bb})/2$ and the two shear components $\gamma_1 = -(\Phi_{aa} - \Phi_{bb})/2$ and $\gamma_2 = -\Phi_{ab}$.

Next we consider the quadratic combinations of the derivatives and express them in terms of the unlensed field to lowest order in the shear tensor,

$$\begin{aligned} \mathcal{S} &\equiv 1 - \sigma_{\mathcal{S}}^{-1} [T_x^2 + T_y^2](\boldsymbol{\theta}) \\ &= 1 - \sigma_{\mathcal{S}}^{-1} [(1 + \Phi_{xx} + \Phi_{yy}) \tilde{\mathcal{S}} + (\Phi_{xx} - \Phi_{yy}) \tilde{\mathcal{Q}} + 2\Phi_{xy} \tilde{\mathcal{U}}] \\ \mathcal{Q} &\equiv -\sigma_{\mathcal{S}}^{-1} [T_x^2 - T_y^2](\boldsymbol{\theta}) \\ &= -\sigma_{\mathcal{S}}^{-1} [(1 + \Phi_{xx} + \Phi_{yy}) \tilde{\mathcal{Q}} + (\Phi_{xx} - \Phi_{yy}) \tilde{\mathcal{S}}] \\ \mathcal{U} &\equiv -2\sigma_{\mathcal{S}}^{-1} [T_x T_y](\boldsymbol{\theta}) \\ &= -2\sigma_{\mathcal{S}}^{-1} [(1 + \Phi_{xx} + \Phi_{yy}) \tilde{\mathcal{U}} + \Phi_{xy} \tilde{\mathcal{S}}], \end{aligned} \quad (2)$$

where $\sigma_{\mathcal{S}}$ was defined so that in the absence of lensing $\langle \mathcal{S} \rangle = \langle \mathcal{Q} \rangle = \langle \mathcal{U} \rangle = 0$. In the presence of lensing it follows

from above $\langle \mathcal{S} \rangle = 2\kappa$, $\langle \mathcal{Q} \rangle = 2\gamma_1$, $\langle \mathcal{U} \rangle = 2\gamma_2$. Physically, κ stretches the image and makes the derivatives smaller. Similarly, shear produces anisotropy in the derivatives and can be extracted by considering the particular combination of derivatives defined above. From \mathcal{Q} and \mathcal{U} we can form two rotationally invariant quantities in Fourier space

$$\begin{aligned} \mathcal{E}(\mathbf{l}) &\equiv \mathcal{Q}(\mathbf{l}) \cos(2\phi_{\mathbf{l}}) + \mathcal{U}(\mathbf{l}) \sin(2\phi_{\mathbf{l}}) \\ \mathcal{B}(\mathbf{l}) &\equiv \mathcal{Q}(\mathbf{l}) \sin(2\phi_{\mathbf{l}}) - \mathcal{U}(\mathbf{l}) \cos(2\phi_{\mathbf{l}}). \end{aligned} \quad (3)$$

The average of the scalar field \mathcal{E} is $\langle \mathcal{E} \rangle = 2\kappa$. The average of the pseudo-scalar field \mathcal{B} vanishes in the large scale limit because gravitational potential from which shear is generated is invariant under the parity transformation. The convergence κ can be reconstructed in two independent ways, either from \mathcal{S} or \mathcal{E} , while \mathcal{B} can serve as a check for possible systematics.

The convergence κ can be written as a projection of gravitational potential $\kappa = \int_0^{\chi_0} g(\chi, \chi_0) \nabla^2 \phi(\chi) d\chi$ [4,5]. Here χ_0 is the comoving radial coordinate at recombination and g is the radial window, defined as $g(\chi, \chi_0) = \frac{r(\chi)r(\chi_0 - \chi)}{r(\chi_0)}$. Here $r(\chi)$ is the comoving angular diameter distance, defined as $K^{-1/2} \sin K^{1/2} \chi$, χ , $(-K)^{-1/2} \sinh(-K)^{1/2} \chi$ for $K > 0$, $K = 0$, $K < 0$, respectively. The curvature K can be expressed using the present density parameter Ω_0 and the present Hubble parameter H_0 as $K = (\Omega_0 - 1)H_0^2$. In general Ω_0 consists both of matter contribution Ω_m and cosmological constant term Ω_{Λ} .

The angular power spectrum of convergence $C_l^{\kappa\kappa}$ has ensemble average [5]

$$C_l^{\kappa\kappa} = \frac{9}{4} \Omega_m^2 \int_0^{\chi_0} \frac{g^2(\chi, \chi_0)}{a^2(\chi)r^2(\chi)} P_{\delta} \left(k = \frac{l}{r(\chi)}, \chi \right) d\chi, \quad (4)$$

where $a(\chi)$ is the expansion factor and we used Poisson's equation to express the convergence directly in terms of time dependent matter power spectrum $P_{\delta}(k, \tau)$. Figure 1 shows the contribution of the 3-d power spectrum $P_{\delta}(k)$ to $C_l^{\kappa\kappa}$ as a function of k for different l . It is a relatively broad function of k . Different cosmological models give somewhat different correspondence between l and k , but in general $l = 10$ probes scales around $\lambda = 2\pi/k = 1h^{-1}\text{Gpc}$, while $l = 1000$ contribution probes scales around $\lambda = 30h^{-1}\text{Mpc}$. We will see below that this spans the observable range of Planck satellite.

From \mathcal{S} and \mathcal{E} one can form three different angular power spectra, $C_l^{\mathcal{S}\mathcal{S}}$, $C_l^{\mathcal{E}\mathcal{E}}$ and $C_l^{\mathcal{S}\mathcal{E}}$, defined as $C_l^{\mathcal{W}\mathcal{W}} = [\mathcal{W}(\mathbf{l})^* \mathcal{W}'(\mathbf{l}') + \mathcal{W}'(\mathbf{l}')^* \mathcal{W}(\mathbf{l})]/2 \delta_{ll'}$. Their expectation value is $\langle C_l^{\mathcal{W}\mathcal{W}'} \rangle = 4W_l C_l^{\kappa\kappa} + N_l^{\mathcal{W}\mathcal{W}'}$. Here $N_l^{\mathcal{W}\mathcal{W}'}$ are the noise power spectra for \mathcal{S} , \mathcal{E} or their cross-term, while W_l is the window function describing the signal degradation because of finite angular resolution and detector noise [8]. The window changes smoothly from unity at

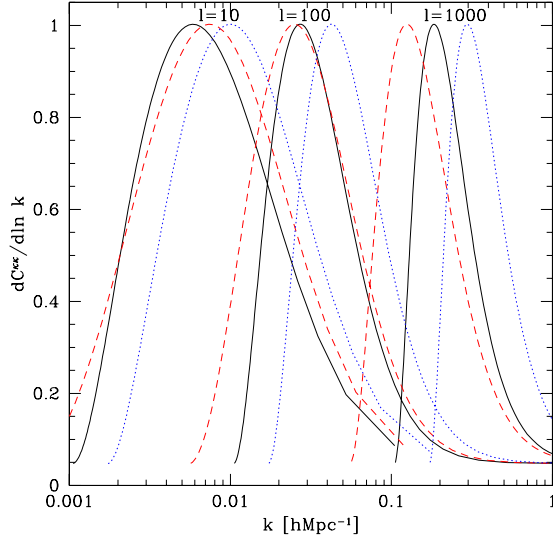


FIG. 1. Logarithmic contribution to $C_l^{\kappa\kappa}$ as a function of k for $l = 10, 100, 1000$ (the normalization is arbitrary). The models are flat CDM model (dotted), open CDM model with $\Omega_m = 0.3$ (dashed) and cosmological constant model with $\Omega_m = 0.3$ (solid). All the models have $\Gamma = \Omega_m h = 0.21$.

low l to zero at high l . For MAP the transition occurs at $l \sim 300$, while for Planck the window is close to unity up to $l \sim 1000$. The noise power spectra have contribution from intrinsic CMB fluctuations and detector noise. In the absence of detector noise it is the correlation length of the CMB ξ that governs the amplitude of noise on large scales. Each patch of the sky of size ξ^2 contributes one independent measurement with a variance of order unity. By averaging over many independent patches we can reduce the noise on large scales. Detector noise and beam smoothing degrade this and the CMB field has to be smoothed at the angular scale where the detector noise exceeds the CMB signal [8]. This increases the CMB correlation length and the amplitude of noise power spectrum. Beam and noise characteristics of Planck (0.12° FWHM and $N^{TT} = (0.01\mu K)^2$) make the influence of detector noise negligible, as there is very little CMB power on small scales which are not accessible by Planck. The noise spectra for $\mathcal{S}\mathcal{S}$, $\mathcal{E}\mathcal{E}$, $\mathcal{B}\mathcal{B}$ and $\mathcal{S}\mathcal{E}$ are shown in top of figure 2. On large scales $N^{\mathcal{E}\mathcal{E}} \approx N^{\mathcal{B}\mathcal{B}} \approx N^{\mathcal{S}\mathcal{S}}/2 \gg N^{\mathcal{S}\mathcal{E}}$. Also shown is the typical convergence power spectrum $4C_l^{\kappa\kappa}$, which is significantly below Planck noise for \mathcal{S} or \mathcal{E} . This shows that the reconstruction can only be achieved in a statistical sense by averaging over independent multipole moments. For MAP with 0.21° FWHM and $N^{TT} = (0.11\mu K)^2$ the noise power spectra are a factor of 5 higher than for Planck [8]. From the measured $C_l^{\mathcal{W}\mathcal{W}'}$ we subtract the noise power spectra $N_l^{\mathcal{W}\mathcal{W}'}$ and are left with an estimate of $C_l \equiv 4W_l C_l^{\kappa\kappa}$.

To combine the three estimates of C_l obtained from $\mathcal{S}\mathcal{S}$, $\mathcal{E}\mathcal{E}$ and $\mathcal{S}\mathcal{E}$ correlations in an optimal way, we con-

sider their covariance matrix. If the CMB noise can be considered Gaussian then the covariance matrix for the estimated power spectra can be expressed in terms of the noise power spectra. We have verified using Monte Carlo simulations that the Gaussian approximation is an excellent one in the large scale limit [8], despite the fact that the underlying fields are not Gaussian (they are constructed using squares of the temperature field). This is a consequence of the central limit theorem, as there are many uncorrelated patches that contribute to the low l modes. The diagonal terms of the covariance matrix are given by $\text{Cov}[(C_l^{\mathcal{W}\mathcal{W}'})^2] = \frac{2}{2l+1}(N_l^{\mathcal{W}\mathcal{W}'})^2$ and $\text{Cov}[(C_l^{\mathcal{S}\mathcal{E}})^2] = \frac{1}{2l+1}[N_l^{\mathcal{S}\mathcal{S}}N_l^{\mathcal{E}\mathcal{E}} + (N_l^{\mathcal{S}\mathcal{E}})^2]$. The off-diagonal elements can be ignored compared to the diagonal terms at low l because $N_l^{\mathcal{S}\mathcal{E}} \ll N_l^{\mathcal{S}\mathcal{S}}, N_l^{\mathcal{E}\mathcal{E}}$. The covariance matrix is then diagonal and we can use simple inverse noise variance weighting to find the best combination

$$\hat{C}_l = \sigma_{C_l}^{-2} \sum_{\mathcal{W}\mathcal{W}'=\mathcal{S}\mathcal{S}, \mathcal{E}\mathcal{E}, \mathcal{S}\mathcal{E}} \frac{C_l^{\mathcal{W}\mathcal{W}'} - N_l^{\mathcal{W}\mathcal{W}'}}{\text{Cov}(C_l^{\mathcal{W}\mathcal{W}'})^2}, \quad (5)$$

where $\sigma_{C_l}^{-2} = \text{Cov}^{-1}[(C_l^{\mathcal{S}\mathcal{S}})^2] + \text{Cov}^{-1}[(C_l^{\mathcal{E}\mathcal{E}})^2] + \text{Cov}^{-1}[(C_l^{\mathcal{S}\mathcal{E}})^2]$ is the variance of \hat{C}_l .

The reconstructed average multiplied with W_l^{-1} is plotted in figure 2 for the Planck experiment using one Monte Carlo realization of the sky. We find that the input power spectrum is recovered up to $l \sim 1000$. The ratio between the two, shown in bottom of figure 2, is consistent with unity over this range, while the corresponding ratio for \mathcal{B} is consistent with 0. There is no significant bias in \mathcal{S} , \mathcal{E} or \mathcal{B} .

Note that even for Planck noise is larger than the signal by a large factor, $(S/N)_l^{-1} = N_l^{\mathcal{E}\mathcal{E}}/4W_l C_l^{\kappa\kappa} \sim 10$ around $l \sim 20$ for this model. Therefore we need about $2(S/N)_l^{-2} \sim 200$ modes to reach $S/N = 1$ on the power spectrum and this is only possible if $l > (2/f_{\text{sky}})^{1/2}(S/N)_l \sim 14f_{\text{sky}}^{-1/2}$, where f_{sky} is the sky fraction that is being observed. This means that we cannot successfully recover the power spectrum for $l < 14$ with $S/N > 1$, so the small scale analysis in this paper is adequate. However, the information from low l modes can still be useful. There may be models which predict a large increase in power on very large (Gpc) scales. For such models noise may be below the signal and should give a detectable signal. Also, low l modes can be cross-correlated with other maps to enhance the signal to noise. One example is the CMB itself, where a positive detection would be a signature of a time dependent gravitational potential [10–12].

For MAP the reconstruction above fails to give a positive detection. A more detailed statistical analysis is necessary to asses the signal to noise when all the information is combined. To asses the overall signal to noise we combine the information from all the estimates $X = \sum_l \alpha_l \hat{C}_l$, such that $S/N = \langle X \rangle / \langle X^2 \rangle^{1/2} =$

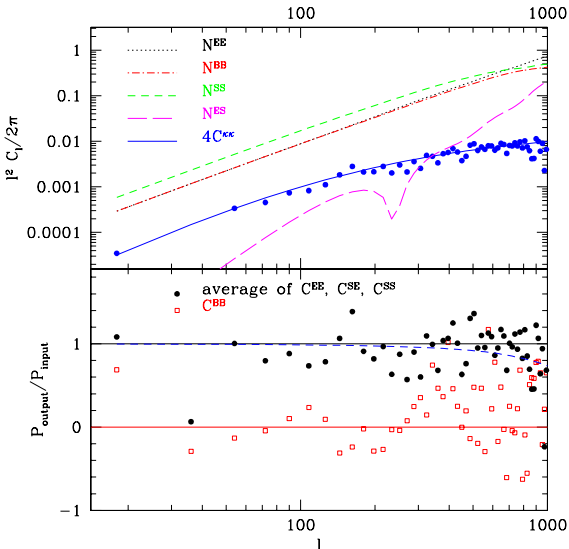


FIG. 2. Top: power spectra for noise N_l^{SS} (short dashed), N_l^{EE} (dotted), N_l^{SE} (long-dashed) and N_l^{BB} (dash-dotted) for Planck, using cosmological constant model with $\Omega_m = 0.3$ and $\sigma_8 = 1$. Also shown is power spectrum of convergence $4C_l^{\kappa\kappa}$ (solid) for the same model, together with its reconstruction from a Monte Carlo simulation. Bottom: ratio of output to input power spectrum is plotted for the averaged $C_l^{\kappa\kappa}$ reconstruction and for the C_l^{BB} reconstruction. Also shown is the window W_l (dashed) for Planck satellite characteristics.

$\sum_l \alpha_l \hat{C}_l / (\sum_l \alpha_l^2 \sigma_{C_l}^2)^{1/2}$ is maximized. This is achieved by $\alpha_l = C_l / \sigma_{C_l}^2$ [10]. The resulting signal to noise is

$$\frac{S}{N} = \left[f_{\text{sky}} \sum_l (2l+1) \frac{16W_l^2 (C_l^{\kappa\kappa})^2}{\sigma_{C_l}^2} \right]^{1/2}. \quad (6)$$

For MAP this gives $S/N = 3$ for $\Omega_m = 0.3$, $\sigma_8 = 1$ model with cosmological constant. Other viable models give comparable numbers. MAP detection will therefore only be marginal, unless the power spectrum on large scales turns out to be much larger than expected. For Planck the viable models give S/N between 15-25, confirming the conclusion above that Planck will be able to extract the power spectrum with high statistical significance.

We have also investigated possible sources of systematics. One is the fact that we have to subtract the CMB noise, which depends on the detailed knowledge of the unlensed CMB power spectrum, while only the lensed power spectrum is known with finite accuracy. We have found both effects to be below 0.5% of the noise amplitude of Planck, so they will not significantly affect the power spectrum reconstruction for Planck, but will be an additional source of error for MAP [8]. Another possible uncertainty is the assumption of the Gaussian statistics, which allows us to estimate the noise and subtract it from the measurements. It should be noted that even if there is a non Gaussian component in the CMB (for example due to foregrounds and secondary processes), the Gaussian

approximation may still be valid on large scales because of the central limit theorem. The accuracy of subtraction is more critical for \hat{C}^{SS} and \hat{C}^{EE} than for \hat{C}^{SE} , where the noise is lower than the signal for $l < 300$ (figure 2). If only cross-correlation is used to estimate $C^{\kappa\kappa}$ then the signal to noise is becomes roughly 2/3 of our previous estimates and would still be clearly detectable with Planck. Finally, there are many consistency checks that can be applied to the reconstruction, such as comparing the three estimators which should all be consistent with each other and verifying that \hat{C}^{BB} is consistent with 0. For low l one may only use \hat{N}^{BB} to subtract the noise directly, as in this limit we have $N^{\text{BB}} = N^{\text{EE}} = N^{\text{SS}}/2$. To summarize, future CMB experiments have the potential of providing another important map of the universe, allowing one to trace the large scale distribution of dark matter to higher redshifts and larger scales than any other method.

U.S. and M.Z. would like to thank Observatoire de Strasbourg and MPA, Garching, respectively, for hospitality during the visits. M.Z. is supported by NASA through Hubble Fellowship grant HF-01116.01-98A from STScI, operated by AURA, Inc. under NASA contract NAS5-26555.

* Electronic address: uros@mpa-garching.mpg.de
 † Address after Feb. 1, 1999: Department of Physics, Jadwin Hall, Princeton University, Princeton, NJ 08544
 ‡ Electronic address: matiasz@ias.edu

- [1] M. Blanton, R. Cen, J. P. Ostriker, M. A. Strauss, submitted to ApJ, astro-ph/9807029 (1998).
- [2] M. A. Strauss, J. A. Willick, Phys.Rept. **261**, 271 (1995).
- [3] R. A. C. Croft, D. H. Weinberg, M. Pettini, L. Hernquist, N. Katz, submitted to ApJ, astro-ph/9809401 (1998).
- [4] R. D. Blandford, A. B. Saust, T. G. Brainerd, & J. V. Villumsen, MNRAS, **251**, 600 (1991); J. Miralda-Escude, ApJ **380**, 1 (1991); N. Kaiser, Astrophys. J. **388**, 272 (1992).
- [5] B. Jain, and U. Seljak, Astrophys. J. **484**, 560 (1997).
- [6] L. Van Waerbeke, F. Bernardeau, Y. Mellier, submitted to A&A, astro-ph/9807007 (1998).
- [7] The gravitational lensing effect on the CMB has been investigated before, e.g. Bernardeau, F., Astron. & Astrophys. **324**, 15 (1997); *ibid.* astro-ph/9802243.
- [8] M. Zaldarriaga and U. Seljak, in preparation (1998).
- [9] D. J. Eisenstein, W. Hu, M. Tegmark, submitted to ApJ, astro-ph/9807130 (1998).
- [10] U. Seljak, and M. Zaldarriaga, to be submitted (1998).
- [11] D. Spergel and D. Goldberg, to be submitted (1998).
- [12] R. G. Crittenden and N. G. Turok, Phys. Rev. Lett. **76**, 575 (1996).